Efficient Apodized-TFBG for DWDM Systems

Eman A. Elzahaby*, Ishac L. Kandas
Department of Engineering Mathematics and Physics,
Faculty of Engineering, Alexandria University, Egypt
Alexandria, Egypt
*eman@alexu.edu.eg

Moustafa H. Aly
College of Engineering and Technology, Arab Academy for Science &Technology & Maritime Transport, Egypt
OSA Member
Alexandria, Egypt

***Abstract*—This study is carried out to optimize the tilted fiber Bragg grating (TFBG) performance in the reflection mode. This optimization starts by controlling the tilt angle, that causes an intensive decrease in the full width at half maximum (FWHM) at the expense on the peak reflectivity. Grating tilt angle is compromised at 5° where a mutual point between narrower FWHM and unity peak reflectivity is achieved successfully. Then, different apodization profiles are applied with TFBG that yield a better performance concerning sidelobes. In general, the TFBG shows a better reflection spectrum when compared to regular FBG. The Nuttall apodization achieves the best performance. Asymptotic decay of 17 dB/nm, low main sidelobe strength (MSLS) of -206 dB, and a narrow FWHM around 0.16 nm were achieved.**

Keywords—Gratings, Tilted Fiber Bragg Gratings, Apodization, Sidelobe supression, Optical Communications.

I. INTRODUCTION

Tilted fiber Bragg gratings (TFBGs) support coupling between different modes. Coupling between core mode propagating in forward direction and core mode propagating in backward directions leads to the reflection spectrum. The reflective fiber Bragg grating (FBG) is mainly used in sensing applications and communications systems [1, 2]. Grating of TFBG is tilted relative to the fiber transverse axis [1-4], while grating perpendicular to the fiber axis (with zero tilt angle) is the regular FBG [4].

Since grating strength begins abruptly and ends abruptly, sidelobes appear in reflection spectrum. This causes a multiple reflected signals in the spectrum beside the main reflected one. This leads to a decrease in the device selectivity when used in communications system, and a decrease in the device sensitivity when used as a sensor. To suppress the sidelobes, the envelope of the refractive index change must have a gradual increase from the beginning of grating to the grating center, as well as gradual decrease from the grating center to the exiting end, this envelope know as Apodization.

Many types of apodization profiles were introduced [5-8] to improve the performance of the grating. Choosing the suitable profile depends on the application. To achieve an optimum performance, the peak reflectivity must be near unity with a narrow full width at half maximum (FWHM), very low main sidelobe strength (MSLS), and very high values for both asymptotic decay and sidelobe suppression ratio (SLSR).

The objective of the present work is to control the tilt angle with a suitable apodization profile to fulfill these demands, and specify the pros and cons of each profile. This would be useful in many applications such as Dense Wavelength Division Multiplexing (DWDM) [5]. We focus on the coupling between modes propagating in opposite directions.

A comparison between TFBG and FBG is carried out and the superiority of TFBG over FBG was demonstrated. According to previous studies [5-6], Nuttall apodization profile gives the best profile in case of normal FBG. The achieved reflectivity ~ 0.9 at operating wavelength of value 1550.4 nm with a main sidelobe level around -89 dB and a narrow FWHM of value 0.21 nm. This was achieved for grating length equals 19 mm and change in the refractive index, $\Delta n = 4\times10^{-4}$.

II. MODEL

TFBGs possess a periodic refractive index modulation along the fiber axis, with a certain tilt angle between the grating plane and fiber cross section as shown in Fig. 1. According to the existence of a small tilt angle, coupling can occur between modes propagating in opposite directions. Maximum coupling occurs at certain wavelength which is needed to be reflected (The operating wavelength). Another coupling can be occurred between forward propagating core mode and counter-propagating cladding mode which we do not focus on it here.

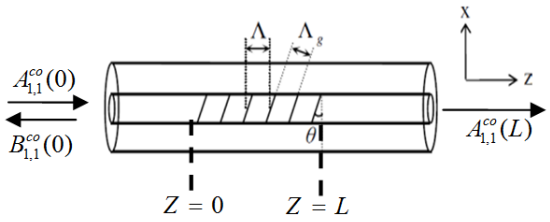

Fig. 1. Schematic of TFBG.

The perturbation of TFBG is identified by [1-4]

$$n(z) = n_{co}[1 + \Delta n\sigma(z)\ cos(2\pi\ z / L)] \quad (1)$$

where $0 < z < L$, L is the grating length, n_1 is the refractive index of the unperturbed core, $\sigma(z)$ is the apodization profile [5-8], Λ is the reference Bragg grating period, Δn is the modulation index amplitude and θ is the grating tilt angle.

Different apodization profiles will be used in this work to optimize the performance of TFBG [5-8],

i) Uniform profile

$$\sigma(z) = 1 \tag{2}$$

ii) Tanh profile:

$$\sigma(z) = tanh\left[\frac{z}{0.32L}\right]^2 \tag{3}$$

iii) Nuttal profile:

$$\sigma(z) = a_o - a_1 cos\left(\frac{2\pi}{L}z\right) + a_2 cos\left(2\frac{2\pi}{L}z\right) - a_3 cos\left(4\frac{2\pi}{L}z\right) \tag{4}$$

where $a_0 = 0.3634$, $a_1 = 0.489$, $a_2 = 0.1365$, and $a_3 = 0.0106$

iv) cos^8 profile:

$$\sigma(z) = \cos^8\left[\frac{2z}{L} - 1\right] \tag{5}$$

For apodized gratings, all profiles are symmetric around the center of the grating and are normalized. Figure 2 shows different apodization functions that are depicted as functions of longitudinal distance, z.

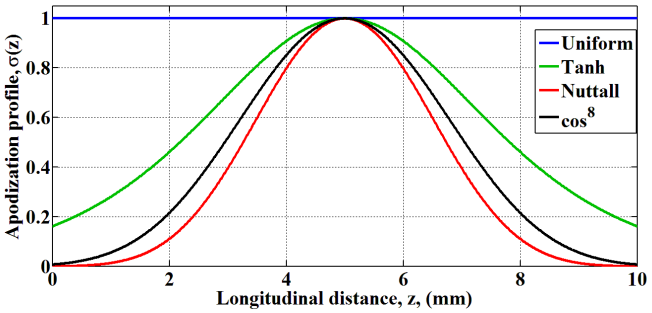

Fig. 2. Apodization functions.

In order to maintain the maximum reflectivity at certain constant value, it is necessary to increase the grating length by a factor $1/a_{eff}$, given by [7]

$$a_{eff} = \frac{L_{eff}}{L} = \frac{\int_0^L z\sigma(z)dz}{\int_0^L z\,dz} \tag{6}$$

where a_{eff} is the apodization paramtere. Table I contains grating length and a_{eff} for different apodization profiles used in this study. Suitable apodization parameters are used to compensate the reduction that occurs in the peak due to apodization. For each apodization profile, the equivalent grating length is determined in order to reach a peak reflectivity of 0.99.

TABLE I EQUIVALENT GRATING LENGTH OF DIFFERENT APODIZATION PROFILES.

FBG Type	a_{eff}	L (mm)
Uniform	1	10
tanh	0.42	23.4
Nuttal	0.36	27.3
cos^8	0.43	23.1

Once the optical fiber is exposed to perturbation on its core refractive index, an exchange of power among guided modes occurs. The coupled mode theory (CMT) provides a simple description of electromagnetic waves propagation and the interaction in perturbed system. The coupled mode equations describe the coupling between core mode propagating in forward direction and the core propagating in the backward direction. They are stated as [2-4, 9-10]

$$\frac{dA_{1,1}^{co}(z)}{dz} = iA_{1,1}^{co}(z) f_{1,1-1,1}^{co-co} + iB_{1,1}^{co} g_{1,1-1,1}^{co-co} e^{-2i\delta_{1,1-1,1}^{r}z} \tag{7}$$

$$\frac{dB_{1,1}^{co}(z)}{dz} = -iB_{1,1}^{co}(z) f_{1,1-1,1}^{co-co} - iB_{1,1}^{co} g_{1,1-1,1}^{-co-co} e^{+2i\delta_{1,1-1,1}^{r}z} \tag{8}$$

where $A_{1,1}^{co}$ is the amplitude of the fundamental core mode in the forward direction and is initially assumed 1 at the beginning of grating, $B_{1,1}^{co}$ is the amplitude of the fundamental core mode in the reverse direction which is assumed to be 0 at the end of grating, $\delta_{1,1-1,1}^{r}$ is the phase matched condition, and $f_{1,1-1,1}^{co-co}$ and $g_{1,1-1,1}^{\pm co-co}$ are the DC and AC coupling coefficients, respectively. Considering the effect of the ultraviolet-induced average index in the core, the phase matched condition can be written as [2-3]

$$\delta_{11-11}^{r} = \beta_{1,1}^{co} - K_g cos\theta + f_{11-11}^{co-co}/2 \tag{9}$$

where $K_g = 2\pi/\Lambda cos\theta$. When $\delta_{11-11}^{r} = 0$, the coupling occurs, then, the position of reflected core mode in the spectrum is determined. This occurs at the Bragg wavelength.

The AC coupling is the response to the sinusoidal change in perturbation Eq. (1). The AC coupling coefficient between the fundamental forward core mode and another core mode propagating in the backward direction is [2-3]

$$g_{1,1-1,1}^{\pm co-co} = \frac{\omega\varepsilon_o n_1^2 \Delta n\ \sigma(z')}{4} \int_0^{a_{co}} \int_0^{2\pi} \left\{ \begin{matrix} E_r^{co-1,1} E_r^{co-1,1*} \\ +E_\phi^{co-1,1} E_\phi^{co-1,1*} \end{matrix} \right\} e^{(\mp 2iK_g r cos\phi sin\theta)} r dr\, d\phi \tag{10}$$

The DC coupling coefficient is the self coupling coefficient that illustrates the coupling coefficient between core/core mode and is defined as [2-3]

$$f_{1,1-1,1}^{co-co} = \frac{\omega \varepsilon_o n_1^2 \Delta n \ \sigma(z')}{2} \int_0^{a_{co}} \int_0^{2\pi} \left\{ \begin{matrix} E_r^{co-1,1} \ E_r^{co-1,1*} \\ + E_\phi^{co-1,1} \ E_\phi^{co-1,1*} \end{matrix} \right\} r dr \ d\phi \quad (11)$$

where ω is the angular frequency, ε_o is the free space permittivity, a_{co} is the core radius, and, are the electric field components of the core mode in the forward direction, respectively [2, 9, 10]. Rung-Kutta method is used to solve the coupled mode equations in order to obtain TFBG spectral response [11]. Then, the reflectivity is calculated from [2-4, 11-13]

$$R = \left| \frac{B_{11}^{co}(0)}{A_{11}^{co}(0)} \right|^2 \quad (12)$$

Once the reflectivity is known, the other evaluation parameters would be calculated. A wide range of evaluation parameters is used to optimize the performance of TFBG. These parameters are summarized in [5-6]. The peak reflectivity occurs at the operation wavelength. The FWHM is defined as the width of the reflected spectrum at half of the maximum power amplitude. MSLS is the amplitude of first main sidelobe. The SLSR is the ratio between the amplitudes of last and first sidelobes. The asymptotic sidelobe (SL) decay is the ratio between the difference of the maximum and minimum sidelobes strength, and the covered wavelengths.

III. Results and Discussion

The study is carried out using a variety of controlling parameters such as L, Δn, θ and $\sigma(z')$. First, we introduced analytical study of the effect of grating tilt angle. Then, we applied different apodization profiles, in order to investigate the effect of each profile. The best profile that produced the best performance was chosen.

A. Charaterics of TFBG Reflectivity

In case of TFBG, increasing the tilt angle minimizes the FWHM and sidelobes as shown in Fig.3. Reflectivity as a function of wavelength at different tilt angle was calculated from Eq. (12), and displayed in Fig. 3. When the tilt angle increased, the grating peak reflectivity decreased. Consequently, it is worth to mention that, the more the tilting of the grating, the less of the light which would be reflected. The used parameters are: L = 10 mm, Δn = 2×10^{-4} and Λ = 0.53 µm. The grating is written on a single mode fiber with core refractive index, n_{co} = 1.44792, cladding refractive index, n_{cl} = 1.44, surrounding medium refractive index, n_s =1, core radius, a_{co} = 2.625 µm, and cladding radius, a_{cl} = 62.5 µm. The apodization is uniform with amplitude 1.

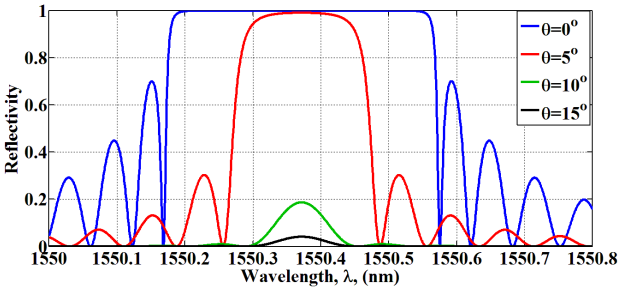

Fig. 3. Reflectivity spectra for tilted grating at different tilt angles.

Comparison is established to judge whether the effect of tilt angle is positive or negative. According to Table II, as tilt angle increase, all evaluation parameters exhibit positively except the peak reflectivity.

TABLE II CHARACTERISTICS OF REFLECTIVITY SPECTRA FOR DIFFERENT TILT ANGLES.

Tilt angle, θ	Peak reflectivity	FWHM (nm)	MSLS (dB)	SLSR (%)	Asymptotic Decay (dB/nm)
0°	1	0.36	-4.3	1.5	27
5°	0.99	0.18	-13	1.8	30
10°	0.16	0.06	-48.2	2.4	32
15°	0.034	0.05	-62	3.3	32.3

Figure 4 shows that both maximum reflectivity and FWHM depend strongly on the tilt angle. FWHM has lower values at $\theta \geq 8°$, while the maximum reflectivity reaches 1 for tilt angle < 5° then its value changes periodically till vanishes for larger values of θ.

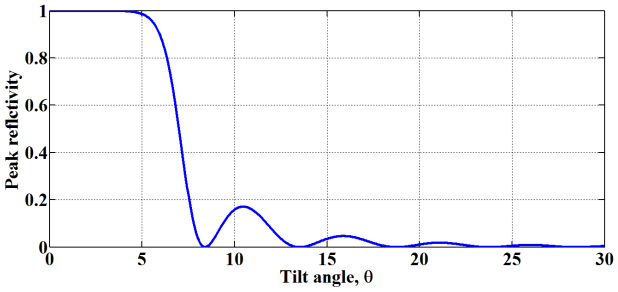

(a)

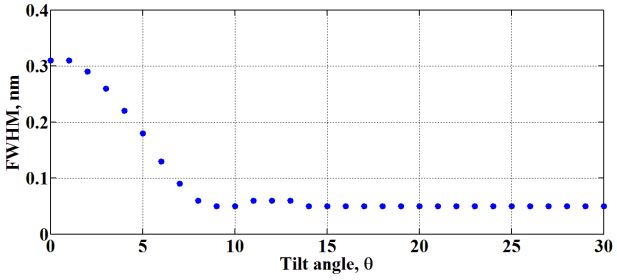

(b)

Fig. 4. (a) Maximum reflectivity and, (b) FWHM as function of tilt angle.

The nulls in maximum reflectivity appear at different tilt angles as shown in Fig. 4a. This relation is similar to the effects of grating tilt angle, θ on AC coupling coefficients between core-mode to core-mode depicted in Fig.5. For θ = 0°, the coupling strength is maximum. Then, as the grating tilt angle, θ increases, the value of coupling decreases till θ ~ 7°. Then, the coupling strength changes periodically till vanishing for larger θ. The change in both Fig. 4a and Fig. 5 depends mainly on the relation between coupling coefficients and the tilt angle described in Eq. (10).

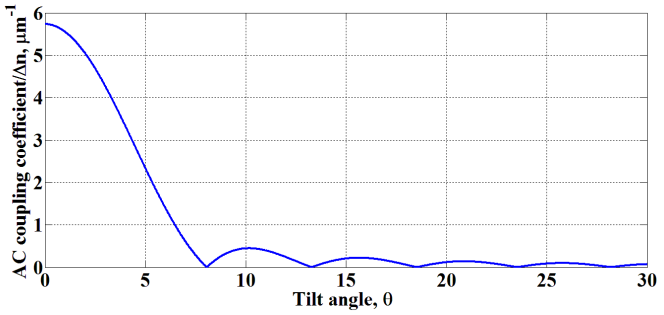

Fig. 5. Variation of noramlized AC coupling coefficients versus grating tilt angle.

The peak reflectivity can be enhanced by increasing the index modulation amplitude or the grating length. Figure 6 shows that the maximum reflectivity for grating with a tilt angle < 5° can reach the maximum value quickly at grating with relatively low length, and index modulation and the opposite for large tilt angle.

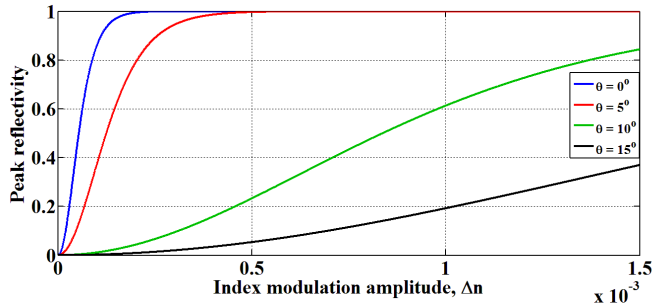

(a)

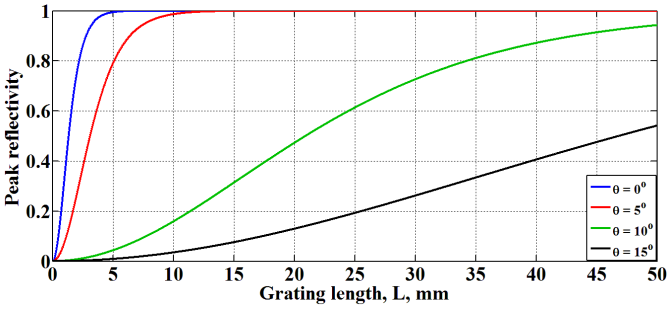

(b)

Fig. 6. Peak reflectivity at different tilt angle as a function of : (a) Index modulation amplitude for grating Length, L = 10 mm, and (b) Grating length for index modulation, $\Delta n = 4\times10^{-4}$.

B. *Apodization effect on the TFBG reflectivity*

The main target of this work is to optimize TFBG by using a suitable tilt angle and a suitable apodization profile. From the previous section, one can concluded that grating with 5° tilt angle is the efficient choice, as the peak reflectivity is kept around 1. Hence, there is no need to increase the grating length or the index modulation.

Now, we apply different apodization profiles to improve the characteristics of reflectivity spectrum. The effect of apodization profiles given by Eqs. (2-5) is shown in Fig. 7. The used parameters are : $\Delta n = 2\times10^{-4}$, L = 10 mm, Λ= 0.53 μm, and θ = 5°.

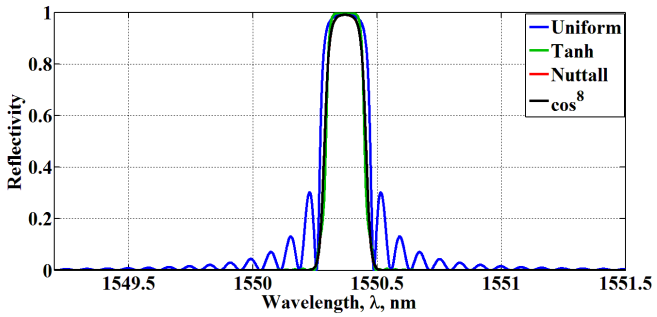

(a)

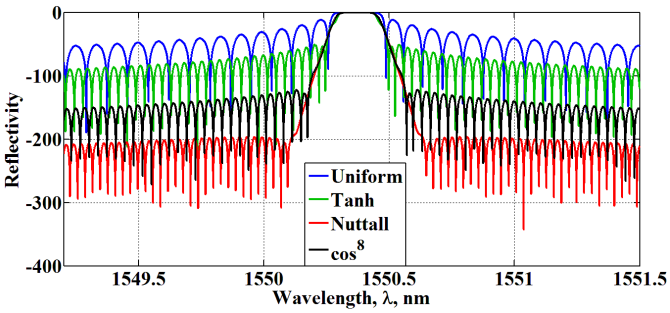

(b)

Fig. 7. TFBG reflectivity spectra for different apodization profiles: (a) Normal scale (b) Logarithmic scale.

Table III contains the reflectivity features for different apodization profiles considering that the grating length was compensated to reach a peak reflectivity of 0.99.

TABLE III CHARACTERISTICS OF REFLECTIVITY SPECTRA FOR DIFFERENT APODIZATION PROFILES.

FBG Type	FWHM (nm)	MSLS (dB)	SLSR (%)	Asymptotic Decay (dB/nm)
Uniform	0.20	-11.93	3	39.9
Tanh	0.15	-53.44	22.5	36
Nuttal	0.16	-206.2	20	17
$\cos^8$	0.16	-127	16	29.45

It is clear that, the Nuttall and cos^8 apodization profiles achieve the better performance. The Nuttall apodization profile achieves a narrow FWHM of 0.16 nm, a lower MSLS of −206

dB, a relative low asymptotic decay of 17 dB/nm, and finally a relative high SLSR of 20 %. The cos^8 apodization function provides a lower MSLS of -126 dB, and a relative high asymptotic decay of 29 dB/nm, but the other parameters do not fit well. The tanh profile introduces the narrower FWHM (0.15 nm) and high SLSR of 22 %, but, unfortunately, the MSLS evaluation parameter is out of competition with the other two apodization profiles. So, one can conclude that Nuttall shows a remarkable performance with TFBG. In previous studies [5-6], the Nuttall profile also provides the best performance with FBG.

A comparison is made in Fig. 8 between FBG and TFBG with $\theta = 5^o$ using the Nuttall profile. For TFBG, the main sidelobe level is -206 dB, and the FWHM is 0.16 nm, while for the regular FBG, the main sidelobe level is -178 dB, and the FWHM is 0.34 nm. The required length of TFBG and FBG is 27.7 mm to obtain the peak reflectivity ~ 1 at $\Delta n = 2\times10^{-4}$.

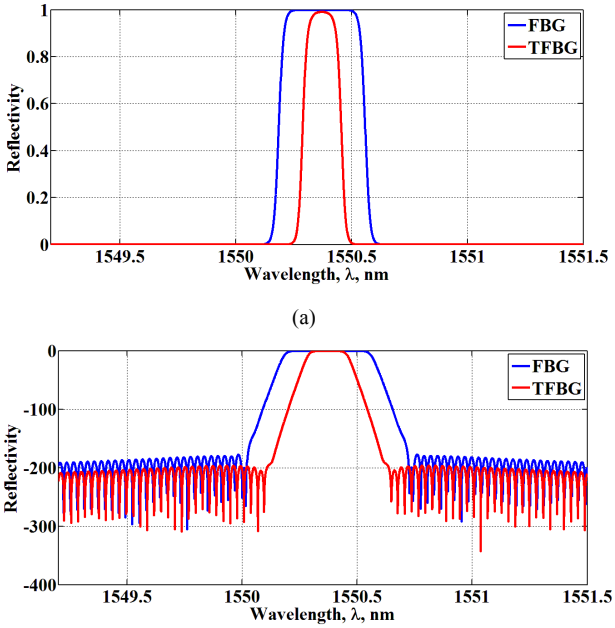

(a)

(b)

Fig. 8. Comparison between TFBG and FBG reflectivity spectra in case Nuttal apodization profile is used :(a) Normal scale (b) Logarithmic scale.

Table IV summarizes the reflectivity features for Nuttall profile for FBG and TFBG at tilt angle 5°.

TABLE IV CHARACTERISTICS OF REFLECTIVITY SPECTRA FOR FBG AND TFBG.

FBG Type	FWHM (nm)	MSLS (dB)	SLSR (%)	Asymptotic SL Decay (dB/nm)
FBG	0.34	-187.5	28	10
TFBG	0.16	-206.2	20	17

IV. CONCLUSION

A design of TFBG is introduced to enhance the performance of the grating in the reflection mode. By controlling the tilt angle, the FWHM decreases in the expense of the maximum reflectivity. The peak reflectivity can be compensated to almost unity by increasing the grating length or the index modulation amplitude.

The grating tilt angle is chosen to be 5° where narrow FWHM and high peak reflectivity are achieved simultaneously. This is carried out for different apodization profiles. On one hand, the performance of Nuttal apodized TFBG with tilt angle, θ = 5° is compared with the regular FBG. FWHM of TFBG is lower than that of TFBG by ~ 47%. MSLS of TFBG is lower than that of FBG by ~ 28 dB. This assures the superiority of TFBG to be used in DWDM systems.

REFERENCES

[1] J. Albert, L. Y. Shao and C. Caucheteur, "Tilted fiber Bragg grating sensors," Laser Photonic Rev., vol. 7, pp. 83-108, 2013.

[2] E. Elzahaby, I. Kandas, M. Aly, K. Mahmoud, "Sensitivity improvement of reflective tilted FBGs," App. Optics, vol. 55, no. 16, 1-7, In Press, 2016.

[3] K. S. Lee and T. Erdogan, "Fiber mode coupling in transmissive and reflective tilted fiber gratings," Appl. Opt., vol. 39, pp. 1394-1404, 2000.

[4] T. Erdogan, "Fiber grating spectra," J. Lightwave Technol., vol. 15, pp. 1277-1294, 1997.

[5] N. Mohammed, T. Ali and M. Aly, "Performance optimization of apodized FBG-based temperature sensors in single and quasi-distributed DWDM systems with new and different apodization profiles," AIP Advances, vol. 3, pp. 1221251-12212521, 2013.

[6] T. Ali, M. Shehata and N. Mohamed, "Design and performance investigation of a highly accurate apodized fiber Bragg grating-based strain sensor in single and quasi-distributed systems," Appl. Opt., vol. 54, pp. 5243-5251, 2015.

[7] K. Ennser, M. Zervas, and R. Laming, "Optimization of apodized linearly chirped fiber gratings for optical communications," IEEE J Quantum Electron., vol. 34, pp. 770-778, 1998.

[8] A. Nuttall, "Some winows with very good sidelobe behavior," IEEE Trans. on Acooustic, Speech, and Signal Prossesing, vol. ASSP-29, pp. 84-91, 1981.

[9] C. Tsao, D. Payne, and W. Alec Gambling, "Modal characteristics of three-layered optical fiber waveguides: a modified approach," J. Opt. Soc. Am. A, vol. 6, pp. 555-563, 1989.

[10] Z. Zhang and W. Shi, "Eigenvalue and field equations of three-layered uniaxial fibers and their applications to the characteristics of long-period fiber gratings with applied axial strain," J. Opt. Soc. Am. A, vol. 22, pp. 2516-2526, 2005.

[11] G. Yin, S. Lou, Q. Li, and H. Zou, "Theory analysis of mode coupling in tilted long period fiber grating based on the full vector complex coupled mode theory," Opt. Laser Technol., vol. 48, pp. 60–66, 2013.

[12] W.-P. Huang and J. Mu, "Complex coupled-mode theory for optical 361 waveguides," Opt. Express, vol. 17, pp. 19134 362 –19152, 2009.

[13] J.-J. Liau, N.-H. Sun, S.-C. Lin, R.-Y. Ro, J.-S. Chiang, C.-L. Pan, and H.-W. Chang, "A new look at numerical analysis of uniform fiber Bragg gratings using coupled mode theory," Prog. Electromagn. Res., vol. 93, pp. 385-401, 2009.